ANOMALOUS IRON DISTRIBUTION IN SHALES AS A MANIFESTATION OF "NON-CLASTIC IRON" SUPPLY TO SEDIMENTARY BASINS: RELEVANCE FOR PYRITIC SHALES, BASE METAL MINERALIZATION, AND OOLITIC IRONSTONE DEPOSITS

Jürgen Schieber

Department of Geology,The University of Texas at Arlington,Arlington, Texas 76019

ABSTRACT

In previous investigations, nearshore pyritic shale horizons in the Mid-Proterozoic Newland Formation were interpreted to be due to "non-clastic" colloidal iron supply by streams. New data on the chemical composition of shales in the Newland Formation support this interpretation. In these shales, Fe and Al show a positively correlated trend that intercepts the Fe axis above the origin. These relationships suggest control of Fe by clays (via iron oxide coatings on clay minerals), and presence of an additional, "non-clastic iron" component. Shales from stratigraphic intervals during which pyritic shale horizons were deposited plot above the Fe/Al trend typical for the remainder of the Newland Formation.

Pyritic shale horizons in sediments are favourable hosts for base metal deposits of the pyrite replacement type. Fe/Al relationships as found in the Newland Formation may help to identify stratigraphic horizons in other sedimentary basins that contain pyritic shale horizons and potentially base metal mineralization.

Introduction

Shales of the eastern Belt basin (Mid-Proterozoic of Montana) contain sizeable horizons of pyritic shale (up to 60m thick, as much as 20 km2 extent, pyrite Fe on the order of several 108 tons; Schieber, 1987, 1989a, 1990). Most of the pyrite occurs as discrete laminated beds, interpreted as mineralized microbial mats.

Study of these pyritic shale horizons (Schieber, 1987), led to the hypothesis that most of the iron was derived from fluvial input in the form of iron colloids (chiefly ferric oxyhydroxides). Iron deposition occurred in partially enclosed coastal embayments (Schieber, 1990), probably due to flocculation caused by mixing with basin waters. An integrated sedimentological and geochemical study (Schieber, 1985) resulted in the hypothesis that pyrite iron was not linked to terrigenous clastic sedimentation (e.g. via iron bearing minerals and oxide coatings on detrital grains), but rather was added as a "non-clastic" sedimentary component ("free" colloidal iron oxyhydroxides). The potential amount of "non-clastic" fluvial iron input was estimated from clues in the sedimentary record (e.g. size of basin marginal drainages, climate, water supply) and the application of knowledge about modern fluvial systems. Even if only very small amounts of "non-clastic iron" (1 ppm or less) are carried in continental waters, the amounts of iron that are supplied to the basin considerably exceed the amounts needed to form the observed pyritic shale horizons (Schieber, 1987).

Studies of modern iron transport to the oceans have documented that most if not all of the fluvial "free" colloidal iron is flocculated in estuaries and nearshore environments (e.g. Boyle et al., 1977; Yan et al., 1991). However, some studies also show iron removal to depend on residence time of water in estuaries, with short residence times allowing for offshore transport of a portion of the "free" colloidal iron (Hong and Kester, 1985). These observations suggest a possible way to test the "non-clastic iron" hypothesis proposed for pyritic shale horizons in the Newland Formation. If they indeed originated through nearshore flocculation of iron colloids, a portion of these might have been carried further into the basin to leave a chemical signal in the accumulating sediments. This possibility is investigated in this paper, and new data are presented to demonstrate "non-clastic iron" supply to sediments of the eastern Belt basin.

Geologic Setting

Pyritic shales occur in two locations along the margins of the Helena embayment (Fig. 1), an

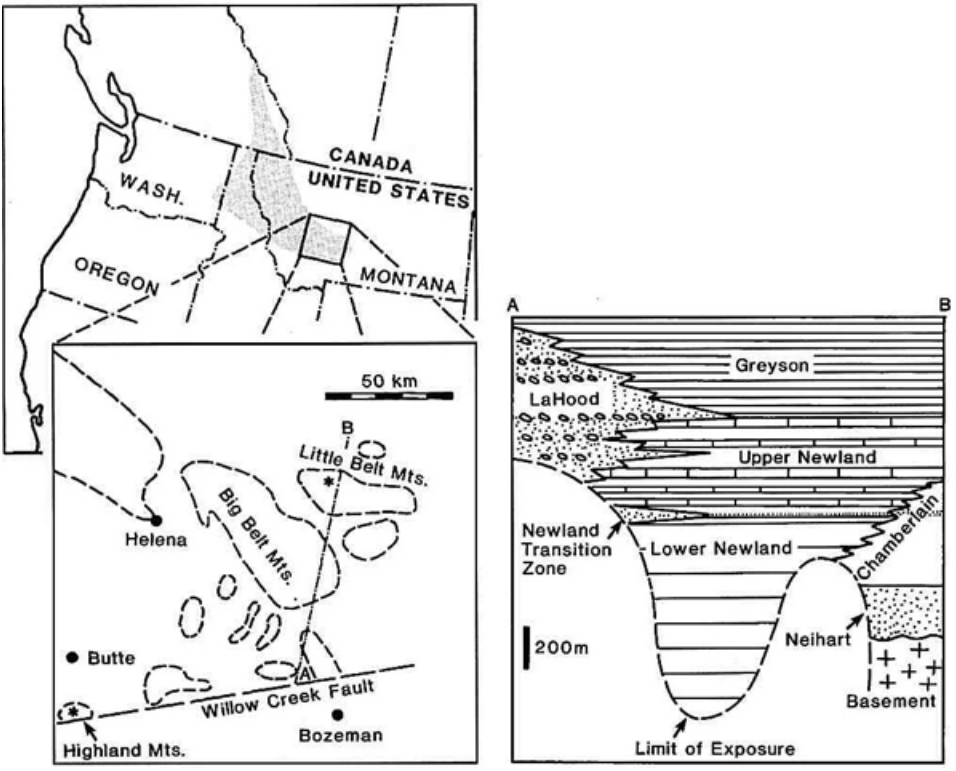

Figure 1: Location map and stratigraphic overview. Stipple pattern indicates present day outline of Belt basin. In enlarged map dashed lines indicate outcrop areas of Belt rocks within the Helena embayment. Star symbols indicate known occurrences of pyritic shale horizons in the Little Belt and Highland Mountains. The stratigraphic overview is based on data from McMannis (1963), Boyce (1975), and Schieber (1985). It represents a generalized restored cross-section along line AB in the enlarged map portion.

eastern extension of the Mid-Proterozoic Belt basin whose sediment fill consists predominantly of sediments of the Lower Belt Supergroup (Harrison, 1972). In the northern Helena embayment pyritic shale horizons occur within the Newland Formation of the southern Little Belt Mountains. They accumulated in coastal embayments that were partially enclosed by offshore sand bars and received terrestrial runoff (details of depositional setting in Schieber, 1990).

The Newland Formation is the most widely exposed stratigraphic unit of the Lower Belt Supergroup in the Helena embayment. It consists of a lower member (dolomitic shales) and an upper member (alternating shale and carbonate packages), as well as of a sandstone bearing transition zone between the two members (also referred to as the Newland Transition Zone or NTZ). In this paper, shale and carbonate packages in the Newland Formation are collectively referred to as Newland shales and Newland carbonates. Pyritic shale horizons of the southern Little Belt Mountains occur in the NTZ (Fig. 1).

Presence of organic matter and pyrite in these sediments indicates anoxic pore waters. Abundant storm layers and carbonaceous shale beds that are probably fossil microbial mats suggest that the Newland Formation did not accumulate under stagnant bottom water conditions (Schieber, 1986b). From age constraints on sediments of the eastern Belt basin (Obradovich and Peterman, 1968; Harrison, 1972), the Newland Formation probably accumulated at a rate of 0.05-0.2 mm/year, and was deposited over a time span of approximately 10-15 m.y. (Schieber, 1987). At the end of Lower Newland deposition the Helena embayment probably changed from a smooth and extensive depression to an east-west trending half-graben with active faults along the southern margin (Schieber, 1985). During NTZ deposition, partially enclosed nearshore lagoons were sites of pyritic shale accumulation (Schieber, 1990), whereas further offshore the shales accumulated that are subject of this study.

Methods of Investigation

Samples of shale (65) and carbonate (23) were collected from the Newland Formation, outside of areas that contained pyritic shales (Big Belt and Little Belt Mountains, Fig. 1). Major element composition of homogenized bulk samples was determined by XRF, following the method of Norrish and Hutton (1969). Duplicate analyses were performed by AA, and some elements (Fe, K, Na) were also checked against INAA data. Data from different analytical methods are in good agreement. Hundreds of thin sections were examined in reflected and transmitted light. A small number of thin sections was examined by electron microscope in secondary (SEM) and backscattered (BSE) mode, and by electron microprobe.

Petrographic Observations

Shales are composed of three principal components, dolomite (in excess of 40 percent in some samples), quartz silt, and clay minerals (primarily illite; XRD data), and consist of interbedded carbonaceous silty shale, dolomitic clayey shale, and siltstone. In siltstone layers, dolomite crystals with rounded impure cores suggest a detrital dolomite component. Detrital silt and mud sized dolomite was probably swept into the basin from dolomitic mudflats along the basin margin (Schieber, 1992a).

Pyrite and organic matter are the most abundant minor components (Py = 1-5.5 volume %; org.-C up to 5 weight %). Pyrite is scattered through the rock as cubic or octahedral crystals (1-20 microns in size) and as framboids (0.1-0.5 mm in size). Although most of the pyrite is of early diagenetic origin (Schieber, 1991; Strauss and Schieber, 1990), pyrite formation continued throughout most of diagenetic history (Schieber, 1991). Pyrite abundance was determined by: (1) visual estimates with comparison charts on polished thin sections (calibrated with point count data); and (2) back-calculating from sulfur analyses of unweathered core material. Both estimates were in good agreement.

Sulfur may also be associated with organic matter (e.g. Raiswell et al., 1993), in which case a determination of pyrite abundance via sulfur analyses would be inaccurate. However, in the study by Raiswell et al. (1993), shales that by organic carbon content are most comparable to those of the Newland Formation (Alum Shales) have nonetheless only a small fraction (2.5%) of their sulfur content in organic matter. Thus, even if some sulfur in the Newland Formation is contained in organic matter, it is probably a safe assumption that the error in the determination of pyrite will not be in excess of a few percent. Furthermore, X-ray dot maps of carbonaceous layers in Newland shales did not reveal noticeable sulfur concentrations outside of pyrite crystals. It seems therefore that pyrite is essentially the only sulfur carrier in these rocks, and that pyrite content can be calculated from sulfur analyses.

Other minerals, micas (muscovite ñ biotite), detrital feldspar, apatite, ilmenite, rutile, zircon, and tourmaline occur in trace amounts only. Together they constitute a few percent of the rock at the most.

Mixing of the three main constituents resulted in shales with considerable compositional variability (dolomite 0-44%, quartz silt content 0-30%, clay minerals 10-60%).

Residence of Iron

Data on iron distribution are from a set of core samples that was investigated in detail. BSE images and X-ray dot maps (Fig. 2) show that (1) the highest iron concentrations are found in pyrite, biotite, and ilmenite; (2) iron contents in dolomite and clay particles are small (ñ uniformly distributed); and (3) quartz, feldspar, and apatite grains are essentially free of iron.

Microprobe analyses of dolomite crystals in six shale samples that span the range from dolomite-poor to

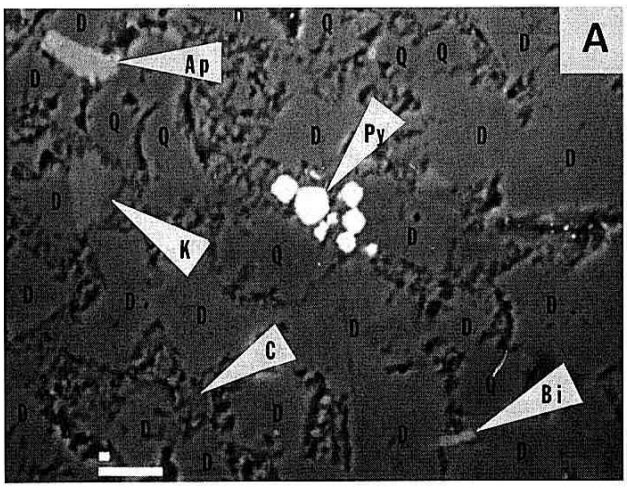

Figure 2a: BSE photograph of dolomitic Newland shale. Minerals are marked as follows: D=dolomite; Q=quartz; bright spots are pyrite (arrow Py); K-spar (arrow K); the rough areas between quartz and dolomite crystals are clay matrix (arrow C); biotite (arrow Bi); apatite (arrow Ap). Scale bar is 10 æm long.

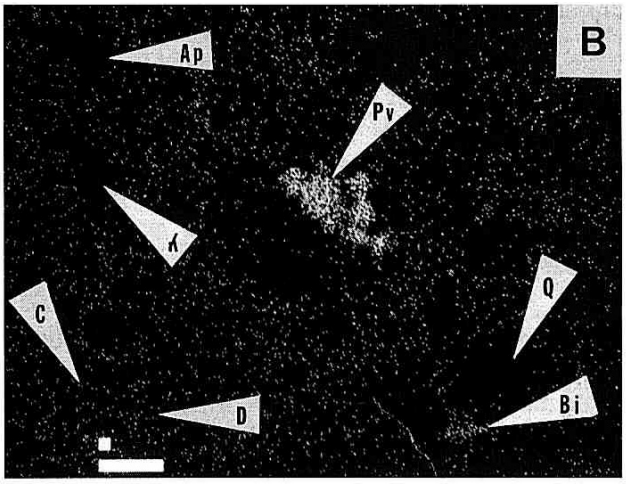

Figure 2b: Iron X-ray dot map of same area as shown in Figure 2a. Note that pyrite has the largest dot density (arrow Py), followed by biotite (arrow Bi). Areas occupied by quartz grains (arrow Q), K-spar (arrow K), and apatite (arrow Ap) show essentially no dots. Dolomite crystals (arrow D) and clay matrix (arrow C) show essentially the same dot density.

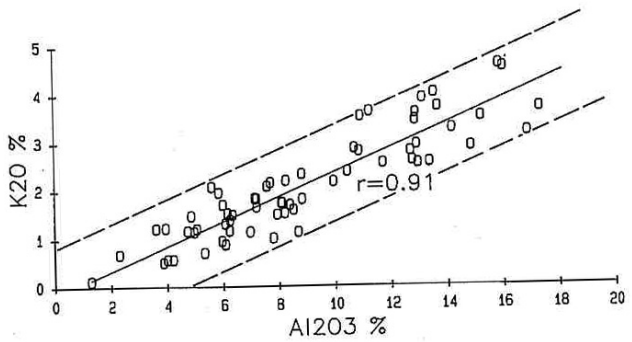

Figure 3: Positive correlation between potassium and aluminum in Newland shales. Solid line marks regression line, slope=0.255, K2O axis intercept=-0.17. Dashed lines delineate compositional trend.

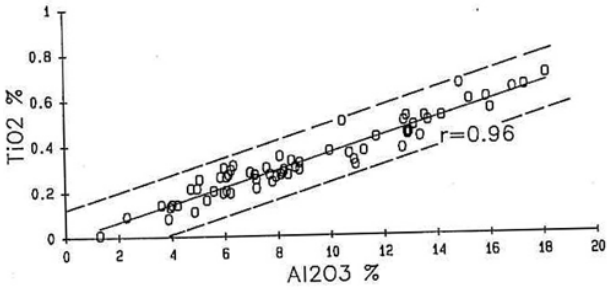

Figure 4: Positive correlation between titanium and aluminum in Newland shales. Solid line marks regression line, slope=0.037, TiO2 axis intercept=-0.007. Dashed lines delineate compositional trend.

dolomite-rich show that their iron content is uniformly low and averages 1.8% Fe2O3. Clay minerals (illite) were too small to be probed individually, but analyses of clay matrix regions (3 micron beam diameter) between dolomite crystals lead to the same average iron content as found for dolomite (1.8%). This result is corroborated by the fact that dolomite crystals and clay matrix regions have essentially the same dot density in Fig. 2.

Calculating pyrite iron via sulfur analyses, one finds that on average two thirds of the total iron (68%) resides in pyrite. Calculation of normative illite and dolomite contents from whole rock data, in combination with an average Fe2O3 content of 1.8% for these minerals, shows that all of the remaining iron can be accounted for as residing in clay minerals and dolomite. The potential contribution of biotite (0.1-

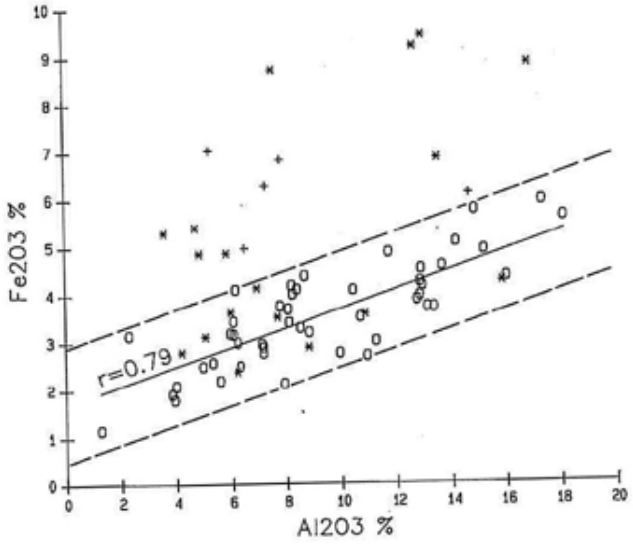

Figure 5: Relationship between iron and aluminum in Newland shales. Samples that are identified with a star are from the NTZ, samples identified with a circle are from above or below the NTZ (lower and upper member of the Newland Formation). The solid line (r=0.79) is a regression line calculated for these samples (slope=0.2: Fe2O3 axis

0.2%) and ilmenite (trace amounts) to the total iron content of the shale is so small that no further consideration is necessary.

Major Element Composition of Shales

Considering that the shales consist primarily of clays, dolomite, and quartz, the bulk of their Al2O3 content obviously resides in clay minerals (primarily illite). Quartz and clay minerals are terrigenous components. Because quartz does not allow incorporation of anything but trace amounts of other elements, examining an elements variability with respect to Al2O3 may reveal how closely its abundance is related to terrigenous clastic sedimentation.

In bulk rock analyses of Newland shales, aluminum shows good positive correlation with potassium and titanium (Figs. 3 and 4), an indication that the latter two elements reside primarily in clay minerals and are a terrigenous clastic component. Scatter in both diagrams can be attributed to small but variable amounts of detrital feldspar and rutile.

Uniform K2O/Al2O3 and TiO2/Al2O3 ratios of these shales may on one hand indicate a source area of similar bulk composition throughout Newland deposition, or on the other hand that original chemical

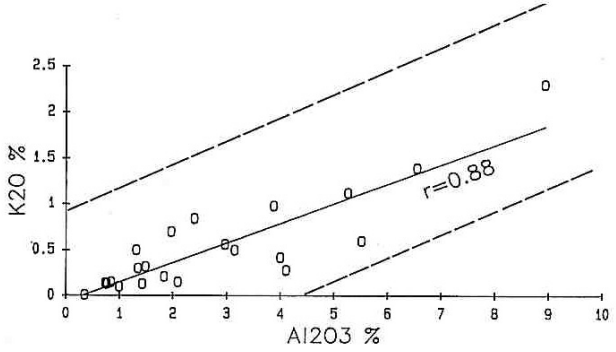

Figure 6: Relationship between potassium and aluminum in Newland carbonates. Solid line marks regression line (slope=0.213, K2O axis intercept=-0.06), the dashed lines are the same that outline the compositional trend for shales in Fig. 3.

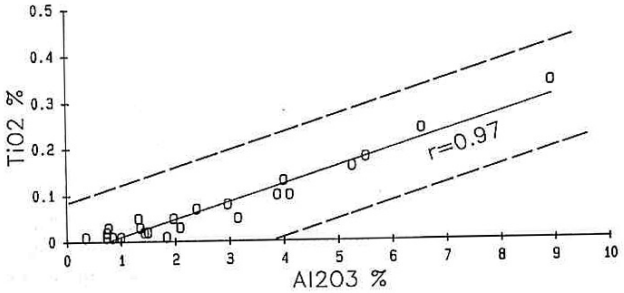

Figure 7: Relationship between titanium and aluminum in Newland carbonates. Solid line marks regression line (slope=0.038, TiO2 axis intercept=-0.027), the dashed lines are the same that outline the compositional trend for shales in Fig. 4.

differences were modified and averaged during diagenetic processes, such as a potential smecitite-illite transformation. The following observations suggest that uniform K2O/Al2O3 and TiO2/Al2O3 ratios are an original feature of these shales:

1) Elements that are commonly considered inert during the sedimentary cycle (e.g. REE's, Th, Hf etc.; Taylor and McLennan, 1985) show little variation in their ratios (Schieber, 1986a, 1992b). Small La/Th ratios and large Hf contents of shales suggest derivation from a crust of largely granitic/granodioritic composition (Bhatia and Taylor, 1981; Condie and Martell, 1983).
2) A petrographic study of sandstones in the Newland Formation suggests that granitoid gneisses and granites

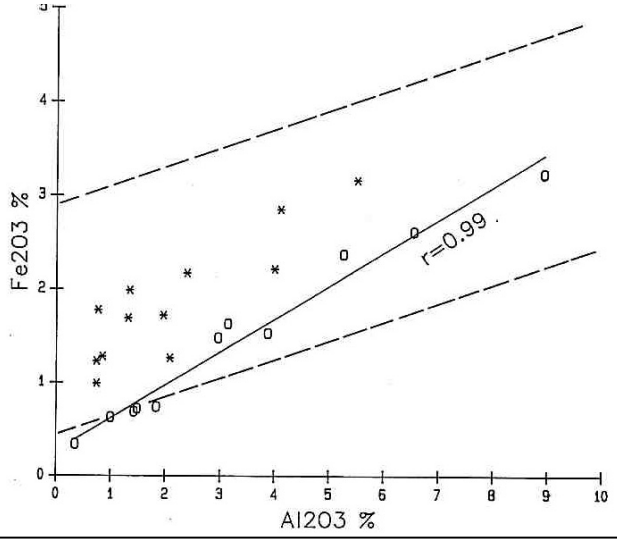

Figure 8: Relationship between iron and aluminum in Newland carbonates. Limestones are indicated by circles, dolomite samples are indicated by star symbols. Solid line marks regression line for limestones (slope=0.353, Fe2O3 axis intercept=0.268), the dashed lines are the same that outline the compositional trend for shales in Fig. 5. It is apparent that the compositional trend of the limestones goes essentially through the origin of the diagram, and that most dolomite samples plot above the limestone trend.

were dominant in the source area of the Newland Formation throughout its deposition (Schieber, 1992b).
3) The generally small permeability of shales makes it appear most unlikely that diagenetic processes could have effectively "erased" previously existing stratigraphic variability of K2O/Al2O3 and TiO2/Al2O3 ratios throughout the whole thickness of the Newland Formation.
4) Large thickness of the Newland Formation (Fig. 1) and the fact that individual shale packages are separated by carbonate units pose further obstacles for wholesale diagenetic homogenization.

In a plot of iron vs aluminum (Fig. 5) the scatter of data points is stronger than in the case of K2O/Al2O3 and TiO2/Al2O3, but a trend of increasing Fe2O3 content with an increase in Al2O3 is visible. The most noteworthy features of Fig. 5 are:

1) Samples from the Lower and Upper Newland Formation (Fig. 1) form a compositional trend

(samples marked as circles in Fig. 5) that intercepts the Fe_2O_3 axis above the origin.
2) Fifty percent of the samples from the Newland Transition Zone (Fig. 1), the stratigraphic interval that hosts pyritic shale horizons (Schieber, 1990), plot above the trend defined by the rest of the Newland Formation (samples marked as stars in Fig. 5).

Manganese shows no systematic relationship to other major elements, probably a reflection of its considerable mobility in sediments. Yet, whereas the great majority of shale samples contains less than 0.1% MnO, a large proportion of samples that come from the NTZ have MnO contents ranging from 0.1-0.64%.

Major Element Composition of Carbonates
Main components of Newland carbonates are calcite, dolomite, clay and quartz (Schieber, 1988). Plots of K_2O and TiO_2 vs Al_2O_3 show the same relationships as the shales (Figs. 6 and 7). Strong similarities with respect to other terrigenous controlled elements (Schieber, 1985) further indicate that terrigenous clastic minerals in carbonates and shales have the same provenance. In comparison to shales, the smaller scatter of data points probably reflects a smaller proportion of feldspar and rutile.
In terms of Fe_2O_3/Al_2O_3 relationships (Fig. 8), the carbonates differ distinctly from shales. Fe_2O_3 increases with Al_2O_3, but there is less scatter of data points and no samples plot above the main trend observed for the shales. If only limestones are considered, a trend emerges that goes through the origin of the diagram. Dolomites and dolomitic limestones plot somewhat above the trend defined by the limestones.
Manganese shows no systematic relationship to other major elements. However, whereas limestones typically contain less than 0.05% MnO, dolomites and dolomitic limestones may contain up to 0.15% MnO.

Discussion
The positive Fe-axis intercept of the Fe/Al trend in Fig. 5 is crucial to the discussion of iron supply to the Newland Formation. In modern ocean sediments that lack significant quantities of iron-bearing detrital minerals (e.g. chlorite, biotite), the bulk of their iron content can be traced to iron oxyhydroxide coatings on clay particles (Carroll, 1958; Berner, 1984). Because of this relationship between clay and iron content, suspended sediments of modern rivers and offshore waters (Yan et al., 1991), as well as modern marine sediments (Moore, 1963), show positive correlation of iron with clay content. Also, compositional trends intersect the origin of iron vs clay plots. Thus, in cases where clays supply the bulk of Al_2O_3, Fe/Al plots should show the same characteristics as iron vs clay plots.
Considering these observations on modern sediments, one might expect to see comparable relationships in shales of the Newland Formation. Thus, the positive axis intercept in Fig. 5 seems anomalous, and four working hypotheses come to mind that might explain the deviation of Fe/Al relationships in Newland shales from expected behaviour. These hypotheses are:

1) Diagenetic redistribution of iron altered original Fe/Al relationships (increase of iron content).
2) Wholesale dissolution of clays caused loss of Al and Si from the system and an increase of Fe/Al ratio.
3) Mixing of three iron bearing detrital minerals, e.g. illite, dolomite, and iron oxide coatings on clays (later transformed to pyrite), produced the observed trend.
4) A "non-clastic iron" component was added to the original sediment at time of deposition.

To start with hypothesis 1): Evidence for diagenetic iron mobility can be found in the form of nodules of pyrite, siderite, and ferroan dolomite. Principal reasons as well as geochemical and observational data suggest that iron migration occurred only over short distances (on the order of mm's to cm's) in the Newland Formation.
Firstly, if iron enrichment in these shales was due to diagenetic redistribution, portions of the shale sequence (and a portion of the samples) should also show signs of iron depletion. However, from Fig. 5 it is obvious that iron enrichment (upward shift of the Fe/Al trend) is the rule.
Secondly, calculations that simulate diagenetic processes in carbonaceous shale (M.H. Reed, personal communication) show that H_2S production (due to presence of organic matter and sulfate) inhibits mobilization of metals. Primarily because metals mobilized from detrital grains are immediately reprecipitated as metal sulfides. Reducing conditions during diagenesis of Newland shales are indicated by the ubiquitous presence of organic matter and formation of pyrite well into late diagenesis (Schieber, 1991). Together with sulfur isotope data that suggest bacterial sulfate reduction as a sulfur source (Strauss and Schieber, 1990), this indicates that the pore waters of these shales contained H_2S for most of their

diagenetic history and precludes any possibility for large scale Fe-migration within the Newland Formation. Textural evidence for diagenetic iron migration and redistribution (e.g. pyrite concretions) was rarely observed in approximately 1000 m of core. Thirdly, the shales typically consist of interbedded layers of carbonaceous silty and dolomitic clayey shale ("striped shales"; Schieber, 1986b, 1989b). Berner (1969) described a comparable experimental setup where an organic-rich layer was in contact with an organic-poor layer. Iron migrated towards the organic-rich layer during early diagenesis, and pyrite formed at the boundary. In striped shales, preferred pyrite deposition near the margin of carbonaceous silty shale layers has not been observed. This suggests that even though the dolomitic clayey shale beds contain only comparatively small amounts of organic carbon (less than 1%, as compared to as much as 5% in carbonaceous silty shale beds), H2S concentrations were sufficient to precipitate in the form of iron sulfides any iron that went into solution during diagenesis. Considering that individual shale beds are on the order of a few mm's to cm's thick, it is then obvious that diagenetic iron redistribution in Newland shales only occurred over very short distances, most likely not in excess of a few mm's to cm's.
Newland carbonates contain similar amounts of organic carbon as the dolomitic clayey shales, and pyrite concretions are rare. It is therefore assumed that they behaved similar to the shales with respect to diagenetic redistribution of iron.

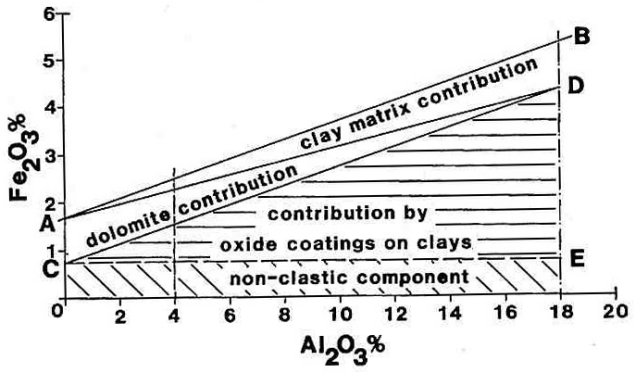

Figure 9: Graphical presentation of iron contribution by various minerals in Newland shales. Line A-B is the regression line from Fig. 5. Contribution by dolomite is indicated by triangle ACD, contribution by clay matrix indicated by triangle ABD. The area below line C-D indicates iron in diagenetic pyrite. Horizontal lined area indicates potential contribution of iron oxides in clay coatings, oblique lined area indicates potential contribution from "non-clastic iron" component.

Finally, even though pyrite concretions were rare, care was taken not to analyse samples with visible concretions in order to minimize possible diagenetic overprint of interelement relationships. Aside of this precaution, samples to be powdered for analysis were subsampled from larger samples as slices perpendicular to bedding, so as to average over as many layers as possible. For above reasons, Fe/Al relationships in whole rock analyses of the Newland Formation should closely resemble bulk Fe/Al relationships in the original sediments.
Regarding hypothesis 2), if wholesale dissolution of clay minerals caused iron enrichment in Newland shales, the effect should be most pronounced in the pyritic shale horizons (described by Schieber, 1990). Because illite, quartz, and dolomite are basic components of the shales, their bulk chemical composition is dominated by SiO2, Al2O3, CaO, MgO, and CO2. The latter three components are almost entirely contained in the dolomite fraction of these shales, and therefore their composition can be represented by a ternary diagram of SiO2, Al2O3, and CaO.
If iron (pyrite) enriched layers in pyritic shales were produced by clay mineral dissolution, the Si/Al, Si/Ca, and Al/Ca ratios of these layers should differ from those of non-enriched shales, and Fe-enriched samples should plot significantly more distant from the Al2O3 pole than unaltered shales. On the other hand, if there was no clay mineral dissolution, pyritic and non-pyritic shales should plot in the same area. The approach just described was used by Croxford (1965) to demonstrate that the Mt. Isa orebodies were of sedimentary (sulfides added as syngenetic sedimentary component) rather than of replacement origin. In the case of the Newland shales, SiO2/Al2O3/CaO relationships reveal no difference between pyritic and "normal" shales (Schieber, 1985). Thus, (1) Fe-enrichment in pyritic shales was not caused by clay mineral dissolution, and (2) the observed relationships suggest that iron was added to these shales as a synsedimentary component. Because pyritic shales in the Newland Formation grade laterally into "normal" shales, it seems likely that the excess iron in "normal" shales is of related origin.
Regarding hypothesis 3), the simple mineralogy of Newland shales, as well as the very small abundance of other iron bearing minerals (biotite, ilmenite), dictates that the observed Fe/Al trend (Fig. 5) has to be explained in terms of contributions by pyrite, dolomite, and clays. Abundant red beds in the Belt Supergroup indicate the presence of oxygen in the atmosphere

(Schidlowski et al., 1975), and iron in surface waters must therefore have been transported in the ferric state. Thus, just as in modern sediments, a large proportion of the iron that was carried into the Belt basin probably travelled originally as iron oxide coatings on clays (Carroll, 1958; Berner, 1984), and was converted into pyrite during diagenesis (Berner, 1970, 1984). As pointed out in the beginning of this discussion, bulk Fe_2O_3 and Al_2O_3 content should in that case show good correlation (Moore, 1963; Yan et al., 1991), and in absence of other iron carriers and aluminous minerals the Fe/Al trend should go through the origin of the Fe vs Al diagram.

Such behaviour is indeed exhibited by limestone samples from the Newland Formation (Fig. 8). Although their Fe and Al resides now in pyrite and clays respectively (Schieber, 1985), the similarity of their Fe/Al relationship to that found in modern sediments (Moore, 1963; Yan et al., 1991) strongly suggests that the bulk of the iron in the limestones was linked to the clay fraction. During diagenesis iron oxide coatings on clays were most likely dissolved and reprecipitated as pyrite (Berner, 1984).

Shales differ from limestones mainly in that they show a shallower slope and a positive Fe-axis intercept of the Fe/Al trend (Fig. 5). Because iron oxide coatings on clay minerals are obviously only part of the story, the influence of other iron-bearing components has to be evaluated. Whereas biotite and ilmenite can be disregarded because of overall small abundance, dolomite and clay matrix contribute noticeably to the iron content of the shales. A graphical illustration of iron contribution by various minerals is shown in Fig. 9, where line A-B represents the average Fe/Al compositional trend (regression line from Fig. 5). The fields for iron contribution by dolomite and clay matrix are constructed by considering two end member shale compositions: (1) a non-dolomitic shale (Al_2O_3 = 18%; approx. 54% illite, 36% quartz, remainder of pyrite, organic matter, and trace minerals), whose clay fraction should contribute approximately 0.97% Fe_2O_3 (illite with 1.8% Fe_2O_3); and (2) a shale at the dolomite-rich end of the spectrum (Al_2O_3 = 4%; approx. 40% dolomite, 43% quartz, 12% illite, remainder of pyrite, organic matter, and trace minerals), whose dolomite and clay fraction should contribute about 0.72% and 0.22% Fe_2O_3 respectively (dolomite with 1.8% Fe_2O_3). Because dolomite and clay matrix have the same average iron content, and because one increases while the other decreases, the result of subtracting their respective contributions (triangle ACD for dolomite, triangle ABD for clays) from the average Fe/Al trend (line A-B) is basically a downward shift of that line by about 1% Fe_2O_3 (line C-D). The remaining iron (area between line C-D and the Al_2O_3 axis) resides essentially in early diagenetic pyrite and for reasons stated above should have been derived from iron oxide coatings on clays. In that case however, and by comparison with modern sediments (Carroll, 1958; Moore, 1963; Yan et al., 1991), we should expect to see line C-D intersect close to the origin of the Fe_2O_3 vs Al_2O_3 diagram in Fig. 9. Instead, the axis intercept is at 0.76% Fe_2O_3 and only the area of triangle CDE can be considered to signify the contribution by iron oxide coatings on clays. Thus, at least 0.76% Fe_2O_3 is still unaccounted for and it is obvious that hypothesis 3 (mixing of iron-bearing detrital minerals) can not produce the Fe/Al relationships observed in Fig. 5.

It should be noted here that the dolomite contribution in Fig. 9 is a maximum estimate. Diagenetic recrystallization of dolomite particles is evident by commonly observed euhedral grain boundaries (Fig. 2a), and it is therefore possible that dolomite picked up portions of its iron content during diagenesis from dissolving iron oxyhydroxides. Thus, it is likely that point C (and the "non-clastic iron" contribution) should actually lie at larger Fe_2O_3 values.

By process of elimination this suggests that hypothesis 4 is indeed viable. Adding a "non-clastic iron" component (iron not associated with detrital particles either as mineral constituent or grain coating) to the normal shales of the Newland Formation would primarily produce an upward displacement of the preexisting detrital Fe/Al trend in an Fe_2O_3 vs Al_2O_3 diagram and could account for the excess 0.76% Fe_2O_3 in Fig. 9.

In earlier papers on pyritic shale horizons of the Newland Formation (Schieber, 1987,1989a, 1990), volcanic emanations (Gole and Klein, 1981) and upwelling of deep ocean waters (Holland, 1973) were eliminated as possible iron sources because of an absence of volcanic rocks in the Lower Belt Supergroup and the paleogeographic setting of the Belt basin (Stewart, 1976; Sears et al., 1978; Piper, 1982; Cressman, 1989). Fluvial iron supply (James, 1954) appeared the most likely source of iron, and a model was arrived at (summarized in introduction) in which iron oxyhydroxides were carried into the basin by continental runoff and flocculated and accumulated in nearshore areas. Colloidal iron oxides and hydroxides were thought the most likely form of "non-clastic iron"

because of presence of free oxygen in the Mid-Proterozoic atmosphere (Schidlowski et al., 1975), and because todays oceans receive most of their "non-clastic" fluvial iron in form of "free" iron colloids (concentrations around 1 mg per litre are not uncommon, Durum et al., 1963; Boyle et al., 1977). Naturally, the same line of reasoning applies regarding the original nature of "non-clastic iron" in Newland shales. Thus, the upwards shift of the Fe/Al trend in Figs. 5 and 9 can now be understood as a basinwide record of fluvial "non-clastic iron" input in form of colloidal iron oxyhydroxides, answering the initial question of this study in the affirmative.

That most of the "free" colloidal iron that is supplied to the oceans by rivers is flocculated in estuaries and nearshore environments (e.g. Boyle et al., 1977; Yan et al., 1991) might be considered as an argument against above scenario. However, in absence of an estuary and estuarine mixing, one should imagine that at least a portion of the iron flocculates can be carried far offshore in river plumes and by basin circulation. The comparatively low density of these floccules is a further argument in favour of their wide dispersion. Studies that show that in estuaries with short water residence times (river discharge large in proportion to estuarine water volume) a portion of the "free" colloidal iron is carried offshore (Hong and Kester, 1985), suggest that the envisioned offshore dispersion of "free" colloidal iron is indeed possible.

That the samples that define the Fe/Al trend in Fig. 5 were collected over a stratigraphic interval of approximately 1000 m, as well as the complete lack of samples that plot below the Fe/Al trend, suggests that such iron input was commonplace throughout deposition of the Newland Formation. That half of the NTZ data points plot significantly above that trend (Fig. 5) suggests that during NTZ deposition "non-clastic" fluvial iron supply significantly exceeded the "background" level that was normal throughout most of Newland deposition.

If we assume that continental drainages supplied "non-clastic iron" in colloidal form to the basin, the amount of colloidal iron input should be linked to the overall amount of freshwater input. In a very crude way, the amount of terrigenous sediment input may be taken as a measure of freshwater input, because the sediment is transported to the basin by fluvial processes. Thus, at times when terrigenous clastic input was at a minimum (e.g. intervals of predominant carbonate deposition) we should expect only minor manifestations of "non-clastic iron" input. This is borne out by Fe/Al data from limestones and dolomites (Fig. 8). Because limestones were deposited mainly in offshore regions, whereas dolomites were deposited in nearshore-lagoonal environments (Schieber, 1992a), the relative iron enrichment in dolomites and dolomitic limestones (Fig. 8) is consistent with a low-level influx of "non-clastic iron" along the basin margins during carbonate deposition.

The relatively large abundance of Mn-anomalous samples in NTZ samples as well as in dolomites and dolomitic limestones, mimics in a general way the behaviour of iron in the Newland Formation. By way of analogy, this may suggest that part of the Mn as well was added to the sediment as a "non-clastic" component. In modern marine sediments it has been noted that up to two thirds of the Mn is associated with iron oxyhydroxides (Chester and Messiah-Hanna, 1970), probably because of similar chemical behaviour under oxidizing conditions (Maynard, 1983) and possibly also because of adsorption processes (Li, 1981). Because of the close association between iron and manganese oxyhydroxides in modern marine waters, the presence of anomalous Mn concentrations in shale samples from the NTZ could be taken as a further indication that iron oxyhydroxides constituted the "non-clastic iron" component in Newland sediments.

Proterozoic basins of Australia contain pyritic shales that show great textural similarity to those of the Newland Formation and contain in several instances large stratiform Pb-Zn deposits (e.g. Mt. Isa, McArthur River etc.). It was pointed out that there is probably no genetic link between occurrence of stratiform Pb-Zn deposits and pyritic shale horizons (Schieber, 1990). However, whereas in the case of syngenetic exhalative base metal sulfide deposition the presence of pyritic shales may indeed be irrelevant, the situation changes when we consider epigenetic replacement deposits. In the past, a number of geologists (e.g. Grondijs and Schouten, 1937; Davidson, 1962; Brown, 1971) have proposed epigenetic pyrite-replacement models to explain stratiform base metal sulfide deposits within pyritic shales. In these models sulfur-poor metalliferous fluids would rise through the sedimentary column, either along faults or fracture zones or also through permeable lithologies. Because base metal sulfides have smaller solubility products than pyrite, the fluids would react with and break down the preexisting pyrite and deposit basemetal sulfides in its place. Thus, pyritic shales generally make good host rocks for epigenetic replacement deposits. Pyritic

shales of the type found in the Newland Formation occur along the basin margins and have a potential to be intersected by basin marginal faults, the conduits for epithermal mineralizing fluids in several other sediment hosted mineral deposits (Gustavson and Williams, 1981), and may therefore be attractive exploration targets. Pyritic shales would not necessarily have to be of microbial mat origin and be of Precambrian age. An alternative origin for large deposits of pyritic shale might for example be flocculation of colloidal iron in low energy nearshore lagoons with reducing bottom sediments. Such deposits could in principle also be Phanerozoic in age. If one were to explore systematically for such replacement deposits, one might as a first step analyse shales throughout a basin to determine the "background" "non-clastic iron" input, and to identify formations with significantly enhanced "non-clastic iron" supply. A few samples of unmineralized shale from the Urquhart Shale near Mt. Isa were analyzed with this thought in mind. These samples are plotted in Fig. 5 and do indeed fall in the field for enhanced iron input. Within such formations, areas where nearshore facies of reducing character are intersected by syndepositional faults should then be searched for presence of pyritic shale horizons. The latter can then be examined for base metal mineralization.

Fluvial iron input in colloidal form has also been envisioned in the case of Phanerozoic oolitic ironstones (Hallam, 1975), but there is no general agreement on that point (Maynard, 1983). Examining the sedimentary sequences that contain oolitic ironstones for signs of "non-clastic iron" input in the same way as was done for the Newland Formation, might shed new light on the origin of oolitic ironstones and may identify those that indeed owe their origin to fluvial iron input.

Conclusion

Addition of "non-clastic iron" ("free" colloidal iron) to sediments of the Newland Formation manifests itself in an upward shift of the Fe/Al trend of shale samples. The shift signifies a "non-clastic" "background" iron component of about 0.76% Fe_2O_3 in these shales. Shales that were deposited during times of increased iron supply (deposition of pyritic shales in the NTZ) show in 50% of all samples iron contents significantly above this "background" trend. Consideration of the oxidation state of the Mid-Proterozoic atmosphere, as well as the observation of higher than average manganese contents with increased "non-clastic iron" contents, suggests that the "non-clastic iron" component was introduced into the basin in form of iron oxyhydroxides.

Because pyritic shales are good host rocks for epigenetic replacement deposits of basemetals, the described characteristics may help to locate stratigraphic intervals in other sedimentary basins that might contain pyritic shale horizons and have enhanced potential for epigenetic basemetal deposits. Application of this approach to sedimentary sequences that contain oolitic ironstones could help to answer the question if riverine colloidal iron was a factor in their formation.

References

Berner, R.: Migration of iron and sulfur within anaerobic sediments during early diagenesis. Amer. J. Sci. 267: 19-42 (1969)

Berner, R.: Sedimentary pyrite formation. Amer. J. Sci. 268: 1-23 (1970)

Berner, R.: Sedimentary pyrite formation: An update. Geoch. Cosmoch. Acta 48: 605-615 (1984)

Bhatia, M.R., and Taylor, S.R.: Trace element geochemistry and sedimentary provinces: Study form the Tasman geosyncline, Australia. Chem. Geol. 33: 115-125 (1981)

Boyce, R.L.: Depositional systems in the LaHood Formation (Belt Supergroup), southwestern Montana. Ph.D. dissertation, University of Texas, Austin, 247 pp. (1975)

Boyle, E.A., Edmond, J.M., and Sholkovitz, E.R.: The mechanism of iron removal from estuaries. Geoch. Cosmoch. Acta 41: 1313-1324 (1977)

Brown, A.C.: Zoning in the White Pine copper deposit, Ontonogan County, Michigan. Econ. Geol. 66: 543-573 (1971)

Carroll, D.: Role of clay minerals in the transportation of iron. Geoch. Cosmoch. Acta 14: 1-27 (1958)

Chester, R., and Messiah-Hanna, R.G.: Trace element partition patterns in North Atlantic deep sea sediments. Geoch. Cosmoch. Acta 34: 1121-1128 (1970)

Condie, K.C., and Martell, C.: Early Proterozoic metasediments from north-central Colorado: Metamorphism, provenance, and tectonic setting. Geol. Soc. Am. Bull. 94: 1215-1224 (1983)

Cressman, E.R.: Reconnaissance stratigraphy of the Prichard Formation (Middle Proterozoic) and

the early development of the Belt basin, Washington, Idaho, and Montana. U.S. Geol. Surv. Prof. Paper 1490: 80 pp. (1989)

Croxford, N.J.W.: Sulphide-sediment relationships at Mount Isa. Nature 206: 1144-1145 (1965)

Davidson, C.F.: The origin of strata-bound sulfide ore deposits (disc.). Econ. Geol. 57: 265-274 (1962)

Durum, W.H., and Haffty, J.: Implications of the minor element content of some major streams of the world. Geoch. Cosmoch. Acta 27: 1-11 (1963)

Gole, M.J., and Klein, C.: Banded iron-formation through much of Precambrian time. J. Geol. 89: 169-183 (1981)

Grondijs, H.E., and Schouten, C.: A study of Mt. Isa ores. Econ. Geol. 32: 407-450 (1937)

Gustafson, L.B., and Williams, N.: Sediment-hosted stratiform deposits of copper, lead, and zinc. Econ. Geol. 75th Anniv. Vol: 139-178 (1981)

Hallam, A.: Jurassic Environments. Cambridge University Press, Cambridge, 269 pp. (1975)

Harrison, J.E.: Precambrian Belt basin of northwestern United States: Its geometry, sedimentation, and copper occurrences. Geol. Soc. Amer. Bull. 83: 1215-1240 (1972)

Holland, H.D.: The oceans: a possible source of iron formations. Econ. Geol. 68: 1169-1172 (1973)

Hong, H., and Kester, D.R.: Chemical forms of iron in the Connecticut River estuary. Coastal and Shelf Science 21: 449-459 (1985)

James, H.L.: Sedimentary facies of iron-formation. Econ. Geol. 49: 235-293 (1954)

Li, Y.H.: The ultimate removal mechanisms of elements from the ocean. Geoch. Cosmoch. Acta 45: 1659-1664 (1981)

Maynard, J.B.: Geochemistry of Sedimentary Ore Deposits. Springer Verlag, New York, 305 pp. (1983)

McMannis, W.H.: LaHood Formation - a coarse clastic facies of the Belt Series in southwestern Montana. Geol. Soc. Amer. Bull. 74: 407-436 (1963)

Moore, R.A..: Bottom sediment studies, Buzzards Bay, Massachusetts. J. sedim. Petrol. 33: 511-558 (1963)

Norrish, K., and Hutton, J.T.: An accurate X-ray spectrographic method for the analysis of a wide range of geological samples. Geoch. Cosmoch. Acta 33: 431-453 (1969)

Obradovich, J.D., and Peterman, Z.E.: Geochronology of the Belt Series, Montana. Canadian J. Earth Sci. 5: 737-747 (1968)

Piper, J.D.A.: The Precambrian paleomagnetic record: the case for the Proterozoic supercontinent. Earth Planet. Sci. Lett. 59: 61-89 (1982)

Raiswell, R., Bottrell, S.H., Al-Biatty, H.J., and Tan, M.MD.: The influence of bottom water oxygenation and reactive iron content on sulfur incorporation into bitumens from Jurassic marine shales. Amer. J. Sci. 293: 569-596 (1993)

Schidlowski, M., Eichmann, R., and Junge, C.E.: Precambrian sedimentary carbonates: Carbon and oxygen isotope geochemistry and implications for the terrestrial oxygen budget. Precambr. Res. 2: 1-69 (1975)

Schieber, J.: The relationship between basin evolution and genesis of stratiform sulphide horizons in Mid-Proterozoic sediments of central Montana (Belt Supergroup). Ph.D. Dissertation, University of Oregon, 811pp. (1985)

Schieber, J.: Stratigraphic control of rare-earth pattern types in Mid-Proterozoic sediments of the Belt Supergroup, Montana, U.S.A.: Implications for basin analysis. Chem. Geol. 54: 135-148 (1986a)

Schieber, J.: The possible role of benthic microbial mats during the formation of carbonaceous shales in shallow Proterozoic basins: Sedimentology 33: 521-536 (1986b)

Schieber, J.: Small scale sedimentary iron deposits in a Mid-Proterozoic basin: Viability of iron supply by rivers. In: P.W.U. Appel and G. LaBerge (Editors), Precambrian iron-formations. Athens, Theophrastus Publications S.A., 267-295 (1987)

Schieber, J.: Redistribution of rare earth elements during diagenesis of carbonate rocks from the Mid-Proterozoic Newland Formation, Montana, U.S.A. Chem. Geol. 69: 111-126 (1988)

Schieber, J.: Pyrite mineralization in microbial mats from the Mid-Proterozoic Newland Formation, Belt Supergroup, Montana, U.S.A. Sed. Geol. 64: 79-90 (1989a)

Schieber, J.: Facies and origin of shales from the Mid-Proterozoic Newland Formation, Belt basin, Montana, U.S.A. Sedimentology 36: 203-219 (1989b)

Schieber, J.: Pyritic shales and microbial mats: Significant factors in the genesis of stratiform Pb-Zn deposits of the Proterozoic? Min. Deposita 25: 7-14 (1990)

Schieber, J.: The origin and economic potential of disseminated Pb-Zn mineralization in pyritic shale horizons of the Mid-Proterozoic Newland Formation, Montana, U.S.A.: Mineralium Deposita 26: 290-297 (1991)

Schieber, J.: Facies and deposition of a mixed terrigenous-carbonate suite in a Mid-Proterozoic epicratonic sea: The Newland Formation, Belt Supergroup, Montana, U.S.A. N. Jb. Geol. Pal. Abh. 184: 155-180 (1992a)

Schieber, J.: A combined petrographical-geochemical provenance study of the Newland Formation, Mid-Proterozoic of Montana. Geol. Mag. 129: 223-237 (1992b)

Sears, J.W., and Price, R.A.: The Siberian connection: a case for Precambrian separation of the North American and Siberian cratons. Geology 6: 267-270 (1978)

Stewart, J.H.: Late Precambrian evolution of North America: plate tectonics implication. Geology 4: 11-15 (1976)

Strauss, H., and Schieber, J.: A sulfur isotope study of pyrite genesis: The Mid-Proterozoic Newland Formation, Belt Supergroup, Montana: Geochimica et Cosmochimica Acta 54: 197-204 (1990).

Taylor, S.R., and McLennan, S.M.: The continental crust: Its composition and evolution. Oxford, Blackwell Scientific Publications, 312 pp. (1985)

Yan, L., Stallard, R.F., Key, R.M., and Crerar, D.A.: Trace metals and dissolved organic carbon in estuaries and offshore waters of New Jersey, USA. Geochimica et Cosmochimica Acta 55: 3647-3656 (1991)